Rate Coefficient Measurements for the Reaction OH + ClO → Products

Carla S. Kegley-Owen,† Mary K. Gilles,* James B. Burkholder, and A. R. Ravishankara*,†

Aeronomy Laboratory, National Oceanic and Atmospheric Administration, 325 Broadway, Boulder, Colorado 80303, and Cooperative Institute for Research in Environmental Sciences, University of Colorado, Boulder, Colorado 80309

Received: February 4, 1999; In Final Form: May 4, 1999

The rate coefficient for the reaction OH + ClO → products (1) was measured under pseudo-first-order conditions in OH. A discharge flow system was used to produce ClO, and its concentration was measured by UV/visible absorption. OH was produced by pulsed laser photolysis of O_3 (or ClO) at 248 nm in the presence of H_2O and was monitored by laser-induced fluorescence. The value of k_1 between 234 and 356 K is given by $k_1(T) = (8.9 \pm 2.7) \times 10^{-12} \exp[(295 \pm 95)/T]$ cm^3 molecule^{-1} s^{-1}, where uncertainties are 95% confidence limits and include estimated systematic uncertainties. Our value is compared with those from previous investigations.

Introduction

The reaction of OH with ClO

$$OH + ClO \rightarrow HO_2 + Cl \quad (1a)$$

$$\rightarrow HCl + O_2 \quad (1b)$$

may play a significant role in the partitioning of chlorine in the upper stratosphere. The conversion of ClO to Cl in reaction 1a propagates ozone destruction via

$$Cl + O_3 \rightarrow ClO + O_2 \quad (2)$$

while reactive chlorine (ClO and Cl) is converted to the reservoir species HCl in reaction 1b. The branching ratios in reaction 1 are of particular importance, since they directly affect partitioning between active and reservoir, HCl and $ClONO_2$, chlorine species in the upper stratosphere. Recently, Dubey et al.[1] performed a box model sensitivity analysis using the currently recommended value[2] of k_1 and found that a 7% branching ratio for channel 1b reduces the modeled [ClO]/[HCl] ratio to that observed in some field studies. Revisions in the value of k_1 and its temperature dependence would change the value of the branching ratio required to bring field observations and model calculations into agreement. Revisions in the overall value of k_1 would also have other consequences to chlorine chemistry.

Previous measurements of k_1 contain discrepancies in both its magnitude and temperature dependence. Determinations of k_1 at room temperature range from 0.91×10^{-11} to 1.99×10^{-11} cm^3 molecule^{-1} s^{-1}.[2] The value of k_1 currently recommended for atmospheric models is $k_1(T) = 1.1 \times 10^{-11} \exp[(120 \pm 150)/T]$ cm^3 molecule^{-1} s^{-1}, with $k_1(298\ \text{K}) = 1.7 \times 10^{-11}$ cm^3 molecule^{-1} s^{-1}.[2] This recommendation is based on the data of Hills and Howard[3] (who observed a negative temperature dependence ($E/R = 235 \pm 46$ K)), of Burrows et al.[4] (who reported no dependence of k_1 on temperature), and the value of Poulet et al.[5] (at 298 K). Previous studies, all of which were carried out under pseudo-first-order conditions in OH, used discharge flow systems for the radical source (or sources) followed by detection of OH via resonance fluorescence, laser-induced fluorescence, or laser magnetic resonance. Several experiments have used reaction 2 with an excess of Cl atoms as the ClO source and assumed that the initial ozone concentration was equal to the initial ClO produced, $[O_3]_0 = [ClO]_0$.[4,6,7] We will examine this assumption in this work. Other experiments done in excess Cl atoms applied corrections[4,5,7] to k_1 to account for the regeneration of OH through the reaction

$$Cl + HO_2 \rightarrow ClO + OH \quad (3a)$$

$$\rightarrow HCl + O_2 \quad (3b)$$

A few studies have used excess O_3, $[O_3] > [Cl]_0$, when employing reaction 2 as the ClO radical source.[3,5,8]

In this paper, we present results from the study of the temperature dependence of the rate coefficient for reaction 1. Reaction 1 was studied under pseudo-first-order conditions in OH. ClO was generated via reaction 2 under conditions where (a) excess O_3 was present or (b) where O_3 was completely depleted during ClO production. In these experiments ClO and O_3 were monitored simultaneously via UV/visible absorption in situ.

Experiments

Owing to the relatively slow self-reaction of ClO and the high sensitivity with which OH can be detected by laser-induced fluorescence, we studied this reaction under conditions of $[ClO] > 10[OH]_0$ (pseudo-first-order in OH). The apparatus used was a combination of a discharge flow system for producing ClO, a UV/visible absorption spectrometer to quantify ClO concentration, and a pulsed laser photolysis and pulsed laser-induced fluorescence system for producing and detecting OH. The apparatus and methods of operation are described in detail in a recent publication.[9]

ClO Production. Cl atoms were generated in a side arm of a flow tube (2.54 cm i.d.) by passing a dilute mixture of Cl_2 in

* To whom correspondence should be addressed. Address: NOAA/ERL, R/E/AL2, 325 Broadway, Boulder, CO 80303. E-mail: Ravi@al.noaa.gov or mgilles@al.noaa.gov.

† Also affiliated with the Department of Chemistry and Biochemistry, University of Colorado, Boulder, CO 80309.

10.1021/jp9904320 CCC: $18.00
Published on Web 06/15/1999

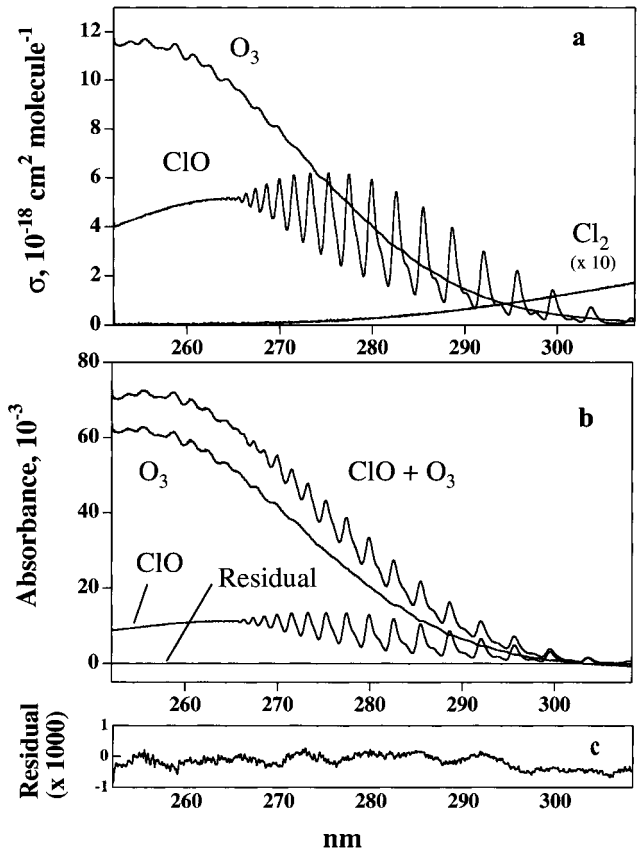

Figure 1. (a) Reference spectra of O_3, ClO, and Cl_2. (b) Example of the spectral subtraction used to obtain [ClO]. (c) Residual (×1000) obtained after subtracting the scaled ClO and O_3 reference spectra from the measured spectrum that contained both ClO and O_3.

He through a microwave discharge. Within the flow tube, Cl atoms reacted with O_3 added through the movable injector via reaction 2, where $k_2(298\ \text{K}) = 1.2 \times 10^{-11}$ cm^3 molecule^{-1} s^{-1}.[2] Typical flow rates of He in the flow tube were 16−38 STP cm^3 s^{-1} at pressures of 4.2−15.4 Torr. This resulted in linear gas flow velocities in the flow tube and reaction cell (also 2.54 cm i.d.) of 330−800 cm s^{-1}. ClO concentrations ranged from 0.3×10^{13} to 12×10^{13} molecule cm^{-3}.

UV Absorption Spectroscopy. The absorbance due to ClO was measured in situ by UV/visible absorption spectroscopy. The output of a 30 W D_2 lamp was collimated and passed through the cell along the axis of the flow (counter to the direction of the photolysis laser beam and perpendicular to the probe laser beam). The D_2 beam was then focused onto the entrance slit of a 0.35 m spectrometer. The spectrometer employed a 600 grooves/mm grating blazed at 300 nm and a cooled 1024 element diode array detector. For monitoring ClO and O_3, the spectrometer was set to observe from 250 to 365 nm at a spectral resolution of 0.8 nm (fwhm). The wavelength was calibrated using the emission lines from a low-pressure Hg lamp. The ClO concentration was quantified using the unstructured portion of its spectrum, since the cross section in this region is well-known and is independent of temperature and resolution.[2] However, the spectral subtraction, discussed later, utilized the structured region of the spectrum.

Reference spectra of O_3, ClO, and Cl_2 are shown in Figure 1 and are in good agreement with literature values.[2] A ClO reference spectrum was measured prior to each experiment by titrating O_3 (or in some cases Cl_2O) with a large excess of Cl atoms. These spectra were recorded under flow, pressure, and temperature conditions that were identical to the subsequent kinetic experiments. The concentration of ClO was calculated using the Beer−Lambert law:

$$A = \sigma l[\text{ClO}] \qquad \text{(I)}$$

where A was the absorbance, σ was the absorption cross section ($\sigma_{253.7\text{nm}} = 4.25 \times 10^{-18}$ cm^2 molecule^{-1}),[2] and l was the path length (28.0−38.8 cm). After each OH temporal profile was recorded, the photolysis laser was blocked and the beam from the deuterium lamp passed through the cell to measure the absorbance due to ClO and O_3. The absorbance due to the initial O_3 could be measured by turning off the microwave discharge. Finally, the flows of O_3 and Cl_2 were shut off and I_0, the intensity in the absence of absorbers, was measured. These spectra were used to determine the initial ozone concentration ($[O_3]_0$) prior to ClO formation, the concentration of ClO, and the concentration of ozone remaining after ClO production, "$[O_3]_{\text{excess}}$". The absorbance due to ClO was extracted from the measured spectrum by subtracting a scaled ClO reference spectrum until all of the ClO structured absorption was completely removed. Since the ClO spectra is structured, this is easily accomplished. The spectral subtraction was normally done by eye immediately after taking the spectra to check for any variation in the deuterium lamp intensity. An example of the spectral subtraction is shown in the lower part of Figure 1. The residual shown in the middle and lower part (×1000) of Figure 1 was obtained by subtracting the remaining O_3. The abundance of ClO (as inferred from its known absorption cross section at 253.7 nm) subtracted from the reference spectra to obtain an unstructured residual was used to determine [ClO]. The concentrations of Cl_2 used, $(0.2-3) \times 10^{14}$ molecule cm^{-3}, were too small to be measured by UV absorption and were calculated from calibrated flows and the total pressure.

Some experiments were carried out under conditions in which ozone was consumed during the ClO radical production. These measurements were performed to test the dependence of k_1 on the presence of excess ozone and the assumption of stoichiometric conversion of O_3 to ClO (reaction 2). Under these conditions, there was no O_3 remaining in the reaction cell. The concentration of remaining Cl atoms was not measured. We could ensure that all O_3 was depleted by comparing the ratio of the measured ClO absorbance under these conditions at 260.0 and 253.7 nm. The absorbance at these two wavelengths for ClO was determined from ClO spectra measured in a large excess of Cl by adding Cl_2O or O_3 to be 1.20 ± 0.01. Because the O_3 cross section[2] at 253.7 nm is ∼2.4 times larger than that of ClO, the ratio would deviate from 1.20 if O_3 were present. Because the measured ratio of absorbance was essentially 1.20, we place an upper limit of 7×10^{11} molecule cm^{-3} of O_3 in the cell.

OH Production. In most experiments, OH was produced via photolysis of O_3 in the presence of H_2O that was added downstream of the flow tube:

$$O_3 + h\nu \rightarrow O(^1D) + O_2 \qquad (4)$$

$$O(^1D) + H_2O \rightarrow 2OH \qquad (5)$$

The rate coefficient[2] for the reaction of $O(^1D)$ with H_2O is $k_5 = 2.2 \times 10^{-10}$ cm^3 molecule^{-1} s^{-1}, and this reaction went to >95% completion in <3 μs. Vibrationally excited OH produced in reaction 5 was quenched rapidly by H_2O. For example, the quenching rate coefficient[10] for OH ($v'' = 1$) by H_2O is 1×10^{-11} cm^3 molecule^{-1} s^{-1} and higher levels are quenched even

faster. With insufficient [H_2O], the vibrational quenching of OH could be observed as a rise in the OH fluorescence signal. Although the exact concentration of H_2O was not needed for the kinetics studies, it was calculated from flows, vapor pressures, and total pressures. H_2O concentrations in the reaction cell were $(3-20) \times 10^{15}$ molecule cm^{-3}. Typical $[OH]_0$ were $(1-3) \times 10^{11}$ molecule cm^{-3} from this OH source. However, in ~10% of the temporal profiles $[OH]_0$ was $\sim 5 \times 10^{11}$ molecule cm^{-3}.

An alternative OH source was the 193 nm photolysis of HNO_3:

$$HNO_3 + h\nu \rightarrow OH + NO_2 \qquad (6)$$

The quantum yield for OH is 0.3 at this wavelength, and the other products are oxygen atoms [$O(^1D) + O(^3P) = 0.8$] and HONO along with very small yields of hydrogen atoms.[11] Initial OH concentrations were calculated to be roughly 6×10^{11} molecule cm^{-3} from the measured photolysis laser fluence, the absorption cross section, and the estimated HNO_3 concentration. For this calculation, we assumed that $O(^1D)$ reacted predominantly with HNO_3 to produce OH, since this would provide an upper limit for $[OH]_0$. $O(^3P)$ would have reacted with ClO, producing Cl atoms that would recycle ClO via reaction with O_3, and HONO would be lost slowly ($k(298\ K) = 4.5 \times 10^{-12}$ cm^3 molecule^{-1} s^{-1})[2] through reaction with OH radicals. Hence, none of the secondary chemistry should have produced OH on a time scale comparable to that for reaction 1. The HNO_3 concentration ($\sim 1 \times 10^{15}$ molecule cm^{-3}) was estimated from the first-order rate constant for OH loss in the absence of ClO due to the reaction

$$OH + HNO_3 \rightarrow \text{products} \qquad (7)$$

which has a rate coefficient of $\sim 1 \times 10^{-13}$ cm^3 molecule^{-1} s^{-1} at 298 K and ~8 Torr.[2]

In experiments where all of the ozone was depleted during ClO production, OH was produced via the 248 nm photolysis of ClO,

$$ClO + h\nu \rightarrow O(^1D) + Cl \qquad (8)$$

followed by $O(^1D)$ reaction with H_2O. The quantum yield[12] for $O(^1D)$ production at this wavelength is ~1. Photolysis fluences were adjusted [(1.5−4.8) mJ pulse^{-1} cm^2] when [ClO] was varied to maintain initial OH concentrations of $(2.9-5.3) \times 10^{11}$ molecule cm^{-3}. ClO concentrations were $10^{13}-10^{14}$ molecule cm^{-3}. We calculated that <2% of ClO was destroyed by photolysis. Hence, photolysis did not significantly affect [ClO].

OH temporal profiles were monitored by laser-induced fluorescence. OH was excited by the frequency-doubled output from a pulsed Nd:YAG pumped dye laser. Fluorescence from the OH ($A^2\Sigma^+$, $v' = 1$) → OH ($X^2\Pi$, $v'' = 1$) and OH ($A^2\Sigma^+$, $v' = 0$) → OH ($X\ ^2\Pi$, $v'' = 0$) transitions passed through a band-pass filter (308 ± 10 nm) and was detected by a photomultiplier tube.[13] Temporal profiles were obtained by varying the delay time between the photolysis and probe lasers from 50 μs to 12 ms.

Because this was the first measurement of an OH reaction rate coefficient on this particular apparatus, we measured the well-known rate coefficient for the reaction

$$OH + CH_4 \rightarrow H_2O + CH_3 \qquad (9)$$

k_9 was measured under pseudo-first-order conditions in OH. $[OH]_0$ (<3×10^{11} molecule cm^{-3}) was produced by pulsed laser photolysis of H_2O_2 at 248 nm. The concentration of CH_4 {$(1-13) \times 10^{16}$ molecule cm^{-3}} was calculated from flow rates and pressure. The value obtained for $k_9(298\ K) = (6.77 \pm 0.26) \times 10^{-15}$ cm^3 molecule^{-1} s^{-1} (uncertainty is 2σ precision) agrees with previous determinations.[2]

Materials. The Cl_2 (1% Cl_2 (>99.99%) in He (>99.997%)), N_2 (>99.9995%), and He (>99.997%) were all obtained commercially. Helium was passed through a liquid nitrogen trap, and all other gases were used as supplied. Ozone was produced in a commercial ozonizer and stored on a silica gel trap kept in a dry ice/ethanol bath. Cl_2O was synthesized following techniques in the literature,[14] and its purity (>92%) was determined via UV absorption. Mass flow controllers were used to measure the gas flows into the cell, and pressure was measured with capacitance manometers. HNO_3 was introduced into the reaction cell by bubbling He through a mixture of concentrated sulfuric and nitric acids.

Results

OH temporal profiles in the presence of excess ClO and O_3 were influenced by the reactions

$$OH + ClO \rightarrow \text{products} \qquad (1)$$

$$OH \rightarrow \text{loss} \qquad (10)$$

where reaction 10 represents the first-order rate coefficient for loss of OH due to diffusion and flow out of the detection region. Other reactions that could influence the OH temporal profile were

$$OH + Cl_2 \rightarrow HOCl + Cl \qquad (11)$$

$$OH + O_3 \rightarrow HO_2 + O_2 \qquad (12)$$

Contributions to the OH loss rate coefficients from reactions 11 and 12 were estimated from the calculated [Cl_2] and measured $[O_3]_{excess}$ along with the respective rate coefficients.[2,15] These losses were estimated to be <1% and <2%, respectively, of the loss due to reaction 1 and were neglected in the data analysis. Normally, $[OH]_0$ was $<5 \times 10^{11}$ molecule cm^{-3} and the loss due to OH self-reaction

$$OH + OH \rightarrow \text{products} \qquad (13)$$

was small. All OH temporal profiles were single exponential decays (see Figure 2) and were fit to

$$\ln[OH]_t - \ln[OH]_0 = -k_1' t \qquad (III)$$

where $[OH]_t$ and $[OH]_0$ represent the OH fluorescence signals at times t and zero, respectively, and $k_1' = k_1[ClO] + k_d$. k_d represents the first-order rate coefficient for reaction 10, reactions with impurities, and reactions 11, 12, and 13. Plots of $\ln[OH]_t$ vs time at 298 K are shown in Figure 2. Values of k_1' were obtained from the slope of such plots determined at various [ClO]. The second-order rate coefficient, k_1, was obtained from the slopes of plots of k_1' vs [ClO] (Figure 3). The intercepts, k_d, from these plots were always within the uncertainty of the OH loss rate coefficients measured in the absence of ClO. Details of the experiments carried out at 298 K in the presence of excess O_3 are given in Table 1.

In some experiments at 298 K done in excess O_3, OH was produced by HNO_3 photolysis at 193 nm (reaction 6). For these

TABLE 1: ClO + OH Experiments at 298 K in the Presence of Excess O_3[a]

OH source	[ClO]	$[O_3]_{excess}$	$[ClO]/[OH]_0$	pressure	v		k_1
$O(^1D) + H_2O$	1.5−8.0	0.24−1.1	60−240	4.2	715		2.56 ± 0.18
	1.4−7.0	0.25−1.4	60−180	7.9	760		2.38 ± 0.14
	1.4−7.0	0.25−1.4	50−240	7.9	760		2.43 ± 0.12
	0.6−8.0	0.8−7.2	70−150	8.4	330		2.49 ± 0.08
	0.6−8.0	0.8−6.5	70−180	8.8	680		2.49 ± 0.16
	1.9−11	0.4−0.8	40−280	8.8	680		2.52 ± 0.18
	2.5−7.2	0.8−20	70−170	15.4	360		2.40 ± 0.31
	3.0−9.0	0.08−0.5	130−760	4.6	790		2.40 ± 0.10
	2.0−9.0	0.09−0.5	90−600	8.2	440		2.41 ± 0.04
	2.0−8.0	1.2−2.3	50−80	7.7	450		2.47 ± 0.14
	2.0−8.3	0.1−0.5	50−150	4.8	770		2.31 ± 0.18
	1.5−8.8	0.1−0.7	40−150	4.7	760		2.30 ±0.10
						average	2.43 ± 0.15
$HNO_3 + h\nu$	1.1−8.7	0.5−1.1	15−100	7.7	350		2.52 ± 0.38
	1.5−7.8	0.6−1.2	10−95	6.5	350		2.42 ± 0.12
	1.9−9.4	0.6−2.4	20−120	8.1	350		2.42 ± 0.24
						average	2.45 ± 0.09

[a] [ClO] is in units of 10^{13} molecule cm^{-3}, $[O_3]_{excess}$ is in units of 10^{14} molecule cm^{-3}, pressure is in Torr, v is in cm s^{-1}, and k_1 is in units of 10^{-11} cm^3 $molecule^{-1}$ s^{-1} with the uncertainty of $\pm 2\sigma$ precision from the fit.

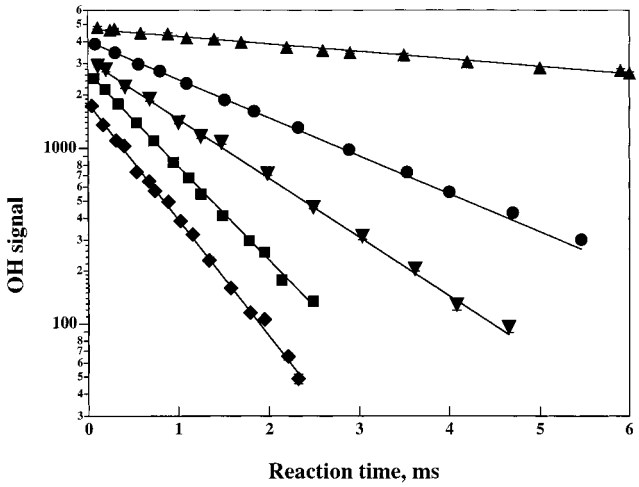

Figure 2. Plots of $\ln[OH]_t$ vs time at 298 K for different ClO under conditions of excess O_3. Values of k_1' were obtained from the slope of such plots at various ClO concentrations.

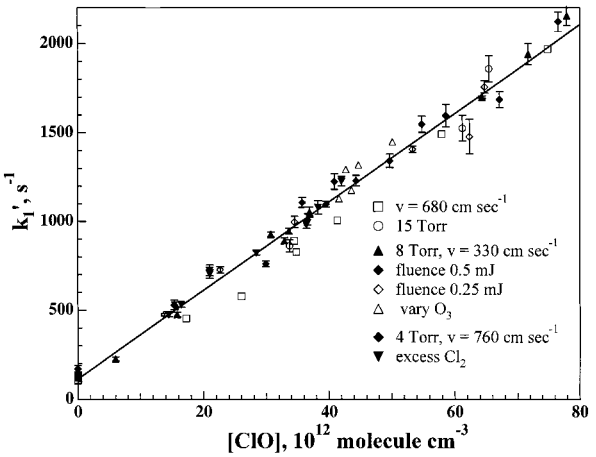

Figure 3. Plot of k_1' vs [ClO], which yields a value for k_1(298 K). These experiments were done under conditions of O_3 (excess). $[O_3]_0$ varied from $(3-40) \times 10^{13}$ molecule cm^{-3}. Measurements were made with different linear gas flow velocities, pressure, and laser fluence as noted in the figure.

experiments the measured k_d also included a loss due to reaction 6, which was used to estimate $[HNO_3]$. The intercepts in the plots of k_1' vs [ClO] were always within the uncertainty of the measured OH loss rate coefficient obtained in the absence of ClO. As seen in Table 1, the rate coefficients determined by producing OH via HNO_3 photolysis in the presence of excess O_3 are in agreement with those obtained using reactions 4 and 5 for OH production.

k_1 was measured at 10 temperatures between 234 and 356 K. At temperatures lower than 234 K, H_2O condensed on the reaction cell surfaces. Experimental conditions and results are summarized in Table 2 and shown in Figure 4. A linear least-squares fit of $\ln k_1$ vs $1/T$ yielded the Arrhenius expression $k_1(T) = (8.9 \pm 2.2) \times 10^{-12} \exp[(295 \pm 65)/T]$ cm^3 $molecule^{-1}$ s^{-1}. The uncertainty in the preexponential factor, A, is $2\sigma_A$ where $\sigma_A = A\sigma_{\ln A}$ and $\sigma_{\ln A}$ is the precision in $\ln A$ from the fit of $\ln k_1$ vs $1/T$. For comparison, the results from previous studies performed in excess O_3 are also shown in Figure 4. The greatest source of possible systematic error in this study involves the determination of the ClO radical concentration. Sources of systematic uncertainties include the absorption cross section of ClO (±5%) and determination of the absorption path length (±3%). Other uncertainties (2σ) arise due to the measurement of temperature (±2 K, which results in an uncertainty of ±1% in [ClO]), loss of OH via reaction with Cl_2 and O_3 (±2%), and the ClO concentration gradient (±5%). The concentration gradient is discussed in detail in prior publications).[9,16] The uncertainty in the spectral subtraction was calculated from 2σ of the mean of the residual absorption (Figure 1c) over the entire wavelength range. This uncertainty was attributed to ClO absorption and used to calculate the percent difference (±6%) in the resulting [ClO]. This is larger than reported in earlier studies because the spectrum of O_3 contains some structure while that of Cl_2O does not.[9] Adding these to the systematic uncertainties gives an overall uncertainty of 22% in [ClO]. Combining this in quadrature with the 2σ precision yields $k_1 = (8.9 \pm 2.7) \times 10^{-12} \exp[(295 \pm 95/T]$ cm^3 $molecule^{-1}$ s^{-1}.

Varying photolysis laser fluence ($0.02-0.5$ mJ $pulse^{-1}$ cm^{-2}) and probe laser fluence (by a factor of 2), increasing $[H_2O]$ $\{(3-20) \times 10^{15}$ molecule $cm^{-3}\}$, and increasing $[O_3]_{excess}$ (a factor of 5) did not affect the measured value for k_1(298 K). In addition, doubling the cell pressure while maintaining a constant flow velocity, and varying the pressure (4.2−15.4 Torr) and flow velocity (330−790 cm s^{-1}) did not affect k_1. Changing the OH source to HNO_3 photolysis and doubling $[HNO_3]$ also had no influence on k_1. Earlier tests on the path length used to determine [ClO] from the absorption measurement are described elsewhere,[9] and additional tests done in the current study are presented in Discussion.

TABLE 2: Determination of k_1 in the Presence of Excess O_3 as a Function of Temperature[a]

T (K)	[ClO]	$[O_3]_{excess}$	$[ClO]/[OH]_0$	pressure	v	photolysis fluence	k_1
234	1.3−12	0.2−1.4	60−150	7.3	460	0.09	3.07 ± 0.16
236	2.0−9.0	2.0−2.7	20−70	7.7	330	0.16	3.24 ± 0.14
236	1.8−5.7	2.0−3.5	60−150	7.7	500	0.06−0.13	2.97 ± 0.08
245	1.6−8.5	0.9−4.9	30−120	7.3	480	0.20	3.24 ± 0.12
252	0.3−8.0	0.3−1.0	80−480	7.3	530	0.08	2.84 ± 0.16
252[b]	1.1−12	0.5−1.4	10−100	7.8	330	0.3	2.74 ± 0.14
263	2.7−8.1	1.8−3.0	20−60	7.5	440	0.21	2.72 ± 0.30
272	1.2−6.7	0.8−2.5	15−420	6.5	410	0.08−0.23	2.77 ± 0.20
298							2.44 ± 0.07
317	1.5−8.0	0.6−2.0	30−200	7.5	440	0.10−0.17	2.22 ± 0.12
336	0.3−7.3	0.8−2.4	20−800	7.3	450	0.19	1.98 ± 0.41
356	1.0−8.0	0.5−1.7	30−100	7.7	430	0.25	1.99 ± 0.12

[a] [ClO] is in units of 10^{13} molecule cm^{-3}, $[O_3]_{excess}$ is in units of 10^{14} molecule cm^{-3}, pressure is in Torr, linear velocity v is in cm s^{-1}, photolysis fluence is in mJ pulse^{-1} cm^2, and $k_1 \pm 2\sigma$ is in units of 10^{-11} cm^3 molecule^{-1} s^{-1}. [b] The OH source was nitric acid photolysis.

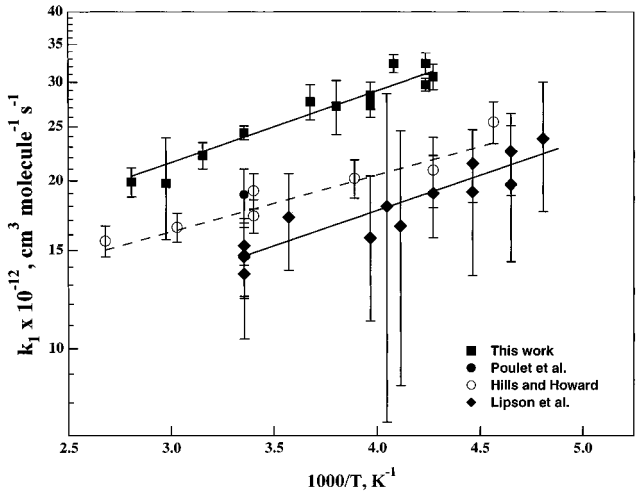

Figure 4. Plots of $k_1(T)$ versus $1000/T$ for experiments done under conditions of excess O_3: this experiment [data (solid squares), fit (solid line)]; Hills and Howard[3] [data (open circles), fit (dashed line)]; Poulet et al.[5] [data (solid circles)]; Lipson et al.[8] [data (solid diamonds), fit (solid line)]. Uncertainties are 2σ precision from the respective papers.

Discussion

There are two categories of potential sources of error in determining k_1 under pseudo-first-order conditions in OH. Side reactions can either increase or decrease the loss rate of OH, resulting in an erroneous value for k_1. In addition, any uncertainty in [ClO] affects the measured rate coefficient. These issues, both in the present and previous experiments, are discussed in this section.

When ClO is made in an excess of Cl, as done in numerous previous experiments, OH is regenerated via reaction 3a.[4−7] The branching ratio for OH production in reaction 3 ranges from 0.01 to 0.28.[17−20] The current recommendation[2] yields a branching ratio of 0.22 for channel 3a.[17] Several previous studies carried out with excess Cl atoms used this value to correct their measured k_1 for OH regeneration.[4,5,7] These corrections to k_1 are significant and ranged from 13 to 30% between 248 and 335 K in the experiments of Ravishankara et al.[7] and from 6 to 13% between 243 and 298 K in those of Burrows et al.[4] and were ∼28% at 298 K in the study of Poulet et al.[5] However, during the experiments of Leu and Lin[6] it was not known that reaction 3 could regenerate OH. Hence, they did not correct their data for reaction 3a and their value for k_1(298 K), 0.91×10^{-11} cm^3 molecule^{-1} s^{-1}, is lower than other determinations. In a number of experiments at 298 K we intentionally depleted O_3 during ClO production and verified that O_3 was depleted using UV/visible absorption. The average of six different k_1' vs [ClO] plots yielded $k_1(298\text{ K}) = (2.28 \pm 0.11) \times 10^{-11}$ cm^3 molecule^{-1} s^{-1} (2σ precision only). These experiments were repeated at 250 and 347 K. Details of the experimental conditions are given in Table 3, and results are shown in Figure 5 along with the Arrhenius expression obtained in excess O_3. These rate coefficients were all slightly lower than those measured in the presence of excess O_3. Since the rate coefficient for reaction 3a, which regenerates OH, increases with increasing temperature, we expected the largest difference at the highest temperatures. At 347 K, k_{3a} is about 25% larger than at 298 K.

TABLE 3: Determinations of k_1 in Experiments Where O_3 Was Depleted[a]

T (K)	[ClO]	$[ClO]/[OH]_0$	pressure	v	photolysis fluence	$k_1(T)$
250	3.0−10	90−105	7.8	430	2.0	2.85 ± 0.08
298	1.6−8.5	80−95	7.4	460	2.2	2.22 ± 0.08
298	2.0−8.0	50−60	7.6	460	1.6−3.5	2.22 ± 0.10
298	1.5−6.0	40	4.8	800	4.8	2.33 ± 0.08
298	0.6−8.0	50	8.8	420	3.5	2.34 ± 0.16
298	3.0−8.0	60	4.4	780	3.0	2.31 ± 0.16
298	4.0−7.4	55	4.4	780	3.0	2.24 ± 0.08
347	1.5−7.7	125	7.7	460	1.5	1.58 ± 0.16

[a] [ClO] is in units of 10^{13} molecule cm^{-3}, $[O_3]_{excess}$ is in units of 10^{14} molecule cm^{-3}, pressure is in Torr, linear velocity v is in cm s^{-1}, photolysis fluence is in mJ pulse^{-1} cm^2, and $k_1(T) \pm 2\sigma$ is in units of 10^{-11} cm^3 molecule^{-1} s^{-1}.

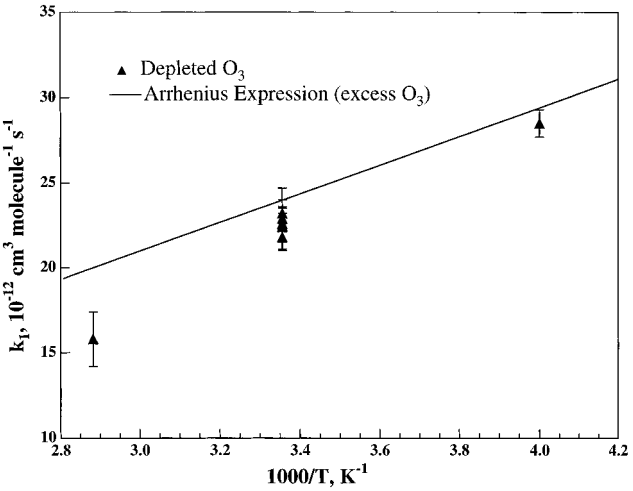

Figure 5. Plot showing the fit to $k_1(T)$ versus $1000/T$ obtained under conditions of excess O_3 (solid line). The filled triangles are data points taken when all ozone was depleted during the production of ClO.

TABLE 4: Facsimile Model Used to Test for Contribution of Reaction 15 to OH Loss[a]

reaction	A^b	E/R
$OH + ClO \rightarrow Cl + HO_2$	8.9×10^{-12}	−295
$OH + Cl_2 \rightarrow HOCl + Cl$	3.8×10^{-12}	1228
$OH + O_3 \rightarrow HO_2 + O_2$	1.6×10^{-12}	940
$OH + HO_2 \rightarrow H_2O + O_2$	4.8×10^{-11}	−250
$HO_2 + ClO \rightarrow HOCl + O_2$	4.8×10^{-13}	−700
$OH + OH \rightarrow H_2O + O$	4.2×10^{-12}	240
$OH + H_2O_2 \rightarrow H_2O + HO_2$	2.9×10^{-12}	160
$OH + HCl \rightarrow H_2O + Cl$	2.6×10^{-12}	350
$OH + HOCl \rightarrow H_2O + ClO$	3.0×10^{-12}	500
$HO_2 + O_3 \rightarrow OH + 2O_2$	1.1×10^{-14}	500
$HO_2 + Cl \rightarrow ClO + OH$	4.1×10^{-11}	450
$HO_2 + Cl \rightarrow HCl + O_2$	1.8×10^{-11}	−170
$HO_2 + HO_2 \rightarrow H_2O_2 + O_2$	2.3×10^{-13}	−600
$Cl + O_3 \rightarrow ClO + O_2$	2.9×10^{-11}	260
$Cl + H_2O_2 \rightarrow HCl + HO_2$	1.1×10^{-11}	980
$Cl + HOCl \rightarrow$ products	2.5×10^{-12}	130
$O + ClO \rightarrow Cl + O_2$	3.0×10^{-11}	−70
$O + HCl \rightarrow OH + Cl$	1.0×10^{-11}	3300
$O + HOCl \rightarrow OH + ClO$	1.7×10^{-13}	0

[a] The first five reactions were used to simulate every OH temporal profile. The remaining reactions were used to test for their influence on the OH loss rate. [b] These are from the Arrhenius expression $k(T) = A \exp[(-E/R)(1/T)]$. A is in units cm^3 molecule^{-1} s^{-1}, and E/R is in K.

In Figure 5 the measured value in the absence of O_3 at the highest temperature is significantly lower than the Arrhenius expression obtained with excess O_3. These experiments were carried out to test if we could observe a different value of k_1 measured in an absence of excess O_3. Since we did not measure [Cl] in these experiments, we cannot correct the measured value of k_1. However, it does show that OH can be regenerated to yield a lower value of k_1 in the presence of Cl atoms.

When k_1 is determined under conditions of excess ozone, OH could be regenerated via

$$HO_2 + O_3 \rightarrow OH + 2O_2 \quad (14)$$

where $k_{14}(298\ K) = 2.0 \times 10^{-15}$ cm^3 molecule^{-1} s^{-1}.[2] In our experiments, $[O_3]_{excess}$ ranged from 8.0×10^{12} to 21×10^{14} molecule cm^{-3} so that reaction 14 should not significantly influence our measured k_1. In previous measurements[3,5,8] of k_1 carried out in excess ozone, $[O_3]$ was sufficiently low that reaction 14 should be negligible.

A secondary reaction that could result in an erroneously large value for k_1 is

$$OH + HO_2 \rightarrow H_2O + O_2 \quad (15)$$

where $k_{15}(298\ K) = 1.1 \times 10^{-10}$ cm^3 molecule^{-1} s^{-1}.[2] Our OH temporal profiles were simulated using FACSIMILE[21] with the reactions shown in Table 4. Only the first five reactions in Table 4 significantly influenced OH temporal profiles under our experimental conditions. Every OH temporal profile was simulated using these five reactions, and $[ClO]_0$, $[O_3]_{excess}$, $[Cl_2]_0$, and $[OH]_0$ were set to match the experimental conditions. To provide a conservative (i.e., largest) estimate of the error and to account for uncertainties in these rate coefficients and in $[OH]_0$, any increase in the OH loss rate due to reaction 15 was doubled. In the majority of the OH profiles loss due to reaction 15 was insignificant (<2% of the OH loss rate due to reaction 1). Although k_1 is about 5 times less than k_{15}, the maximum possible HO_2 concentration was determined by $[OH]_0$, and $[ClO]/[OH]_0$ was always >10, (usually >50). Therefore, HO_2 reacted predominantly with ClO

$$ClO + HO_2 \rightarrow HOCl + O_2 \quad (16)$$

However, the measurements at 324 and 345 K had the largest $[OH]_0$ (and larger uncertainties in $[OH]_0$). At the highest calculated $[OH]_0$, the k_1 measured could be up to 10% larger than the true value because of enhanced OH loss arising from reaction 15. Deleting the data from these two temperatures (along with any other individual measurements of k_1', which could have had >3% contribution due to reaction 15) from the Arrhenius plot yielded $k_1(T) = (8.0 \pm 2.6) \times 10^{-12} \exp[(327 \pm 84)/T]$ cm^3 molecule^{-1} s^{-1} (2σ precision). This value for k_1 is not significantly different from the value for $k_1(T)$ obtained by including these data. Hence, we believe that interference from reaction 15 does not significantly influence our measured value for k_1.

ClO concentrations were $\leq 1.2 \times 10^{14}$ molecule cm^{-3}. Yet, some ClO was lost due to self-reaction:

$$ClO + ClO \rightarrow ClOO + Cl \quad (17a)$$

$$\rightarrow Cl_2 + O_2 \quad (17b)$$

$$\rightarrow OClO + Cl \quad (17c)$$

$$\xrightarrow{M} Cl_2O_2 \quad (17d)$$

where $k_{17}(298\ K) = 2.2 \times 10^{-14}$ cm^3 molecule^{-1} s^{-1} at 8 Torr. Under our experimental conditions (8 Torr, flow velocity of 420 cm s^{-1}, residence time of 80 ms in the absorption/reaction cell) the total decrease in [ClO] across the cell due to self-reaction was calculated to be <12% under conditions of excess O_3 and <30% when O_3 was completely consumed during the formation of ClO. The difference in the ClO loss arises because channels 17a and 17c produce Cl atoms that recycle rapidly to ClO in the presence of O_3. However, the concentration gradient across the length of the absorption cell has little effect on the measured [ClO], since absorption measures a column abundance that, when divided by the path length, yields an average concentration. FACSIMILE[21] simulations and calculations described previously[9,16] show that [ClO] in the reactive volume (intersection of probe and photolysis lasers) located at the midpoint of the absorption cell is the same (within 2% under conditions of excess O_3 and within 11% in the absence of excess O_3) as the integrated column average measured by absorption. Previous tests determining a rate coefficient while measuring [ClO] both prior and after the reaction cell showed that the difference in the determined rate coefficients was consistent with ClO loss via self-reaction alone.[9]

The rate coefficient for reaction 17d, the association reaction to form Cl_2O_2, is greater at lower temperatures. FACSIMILE simulations using reactions 2 and 17 under our experimental conditions showed that at the lower temperatures (234−272 K) and highest ClO concentrations ($\sim 1 \times 10^{14}$ molecule cm^{-3}), $[Cl_2O_2]/[ClO]$ ranged from 0.03 to 0.05. Higher $[Cl_2O_2]$ would have been observable in the absorption spectra; we did not observe any absorption attributable to Cl_2O_2. These $[Cl_2O_2]$ are high enough to possibly affect the OH decay. There are no reported rate coefficients for the reaction

$$OH + Cl_2O_2 \rightarrow \text{products} \quad (18)$$

A value of k_{18} of 5×10^{-11} cm^3 molecule^{-1} s^{-1} would result in an overestimation of our measured k_1 by 10%. However, since all of the k_1' vs [ClO] plots were linear and the $[Cl_2O_2]$ to [ClO]

TABLE 5: Summary of Measurements of k_1[a]

	k_1(298 K)	A	E/R	ClO made w/excess Cl?	corrected for OH regeneration?	assume $[ClO]_0 = [O_3]_0$?
Leu and Lin[6]	0.91 ± 0.26			yes	no	yes
Ravishankara et al.[7]	1.17 ± 0.33	(9.2 ± 6.5)	$-(66 \pm 200)$[b]	yes	yes	yes
Burrows et al.[4]	1.19 ± 0.09	*c*		yes	yes	yes
Hills and Howard[3]	1.75 ± 0.31	(8.0 ± 1.4)	$-(235 \pm 46)$	no	not needed	calibration
Poulet et al.[5]	1.77 ± 0.33			yes	yes	no
	1.99 ± 0.25			yes	yes	no
	1.89 ± 0.21			no	not needed	calibration
Lipson et al.[8]	1.46 ± 0.23	(5.5 ± 1.6)	$-(292 \pm 72)$	no	not needed	no
this work	2.28 ± 0.55			depleted O_3	no[d]	no
	2.44 ± 0.63	(8.9 ± 2.7)	$-(295 \pm 95)$	no	not needed	no

[a] k_1 is in units of 10^{-11} cm^3 molecule^{-1} s^{-1}, A is in 10^{-12} cm^3 molecule^{-1} s^{-1}, and E/R is in K. Uncertainties given are 2σ precision as quoted from the authors, except those of Hills and Howard and ours, which include 2σ precision and estimated systematic uncertainties. [b] Ravishankara et al.[7] measured a negligible temperature dependence and preferred to quote a temperature-independent value. [c] Burrows et al. measured k_1 over the temperature range 243−298 K but reported k_1 as temperature-independent. [d] We were unable to correct for OH regeneration, since we did not measure [Cl].

ratio changes dramatically with [ClO], we believe that the rate coefficient for reaction of Cl_2O_2 with OH is not very large and that our measured rate coefficient is not affected by reaction 18.

Additional tests on the absorption cell path length were also performed. Since the gases flowing through the flow tube and into the absorption/reaction cell may not continuously replenish the extreme ends of the cell (i.e., a stagnant region), we measured an effective absorption cell length *l*. Briefly, a second cell of a fixed path length (50 cm) with no room for stagnation was added in series with the reaction cell. The absorbance of O_3 across both of these cells was measured simultaneously. The $[O_3]$ calculated from the 50 cm long absorption cell was used to obtain *l* of the reaction cell. These cells were attached to one another and had identical diameters; therefore, pressure gradients were <2%. We should note that the difference between the effective path length and simply measuring the entire physical length of the reaction cell was not large, <5%.

Other tests of the path length included adding flush gases at the ends of the reaction cell to ensure that there was no stagnant region and recalibrating the effective path length. In another test, windows were inserted into the absorption/reaction cell to the positions where the flow entered and exited the reaction cell and the physical path length was used. In yet another experiment, the physical path length was increased by 13 cm. For each of these tests k_1(298 K) was remeasured; all of these measurements were within 10% of one another.

Although somewhat redundant, since changes in temperature only change the number density in the reaction cell, we remeasured this path length under each set of temperatures and flow conditions. For each of these temperatures the path length was also calculated using the physical lengths of the sections held at different temperatures (these lengths were obtained by measuring the temperature gradient along the cell). These calculated lengths were within 3% of the calibrated effective path lengths.

On the basis of all these tests, we are confident that [ClO] was determined within 10% if the absorption cross section of ClO at 253.7 nm is exact. The ClO cross section has been measured by many different techniques to obtain the same value (within ±5%). Therefore, we expect our measured [ClO] and k_1 to be accurate.

In kinetic studies of reaction 1 carried out under pseudo-first-order conditions in OH, aside from influences on the OH temporal profiles, any uncertainties in [ClO] or errors in determining [ClO] are reflected in k_1. Some earlier measurements of k_1 generated ClO in an excess of Cl atoms via

$$Cl + O_3 \rightarrow ClO + O_2 \qquad (2)$$

or

$$Cl + Cl_2O \rightarrow ClO + Cl_2 \qquad (19)$$

$[O_3]$ or $[Cl_2O]$ were measured prior to reaction with Cl, and it was assumed that $[ClO]_0 = [O_3]_0$ or $[ClO]_0 = [Cl_2O]_0$.[4,6,7] All of these experiments reported significantly smaller values for k_1 than reported here or by Hills and Howard[3] or Poulet et al.;[5] we believe an overestimation of [ClO] could be the source of this discrepancy. Reaction 2 is very exothermic and can produce vibrationally excited ($ClO^\dagger$). Burkholder et al.[22] observed that as much as 40% of ClO could be lost in excess Cl and suggested that the reaction

$$Cl + ClO^\dagger \rightarrow O + Cl_2 \qquad (20)$$

was responsible for the loss of ClO. Poulet et al.[5] noted ClO losses of up to 50% using reactions 2 and 19 under conditions of excess Cl atoms. Although reaction 19 is not exothermic enough to produce $ClO^\dagger$, the production of Cl_2 was consistent with losses in the injector, most likely because of recombination of ClO (reaction 7).

In our experiments, we determined the concentration of ClO (after its production had gone to completion), the initial concentration of ozone ($[O_3]_0$), and the concentration of any remaining ozone ($[O_3]_{excess}$) by UV/visible absorption. Figure 6a displays a plot of the measured [ClO] vs $[O_3]_0$ obtained under conditions where O_3 was depleted. If the amount of ClO produced were equal to $[O_3]_0$, the data points would fall on the 1-to-1 line. This figure shows that even at low [ClO] the 1-to-1 conversion was not obeyed. The low conversion is consistent with the observations of Poulet et al.[5] and Burkholder et al.[22] over the [ClO] ranges of $(0.25-2.0) \times 10^{13}$ and $(0.4-1.35) \times 10^{13}$ molecule cm^{-3}, respectively. Figure 6b is a plot of [ClO] vs $\Delta[O_3]$ for a few experiments done with O_3 in excess. In both of these types of experiment the conversion efficiency varied depending upon experimental conditions and was somewhat irreproducible. The conversion efficiency may very well change with temperature. The temperature dependence of the conversion efficiency could be one explanation for the discrepancy between those experiments that report a small or no temperature dependence[4,7] and those that report a negative temperature

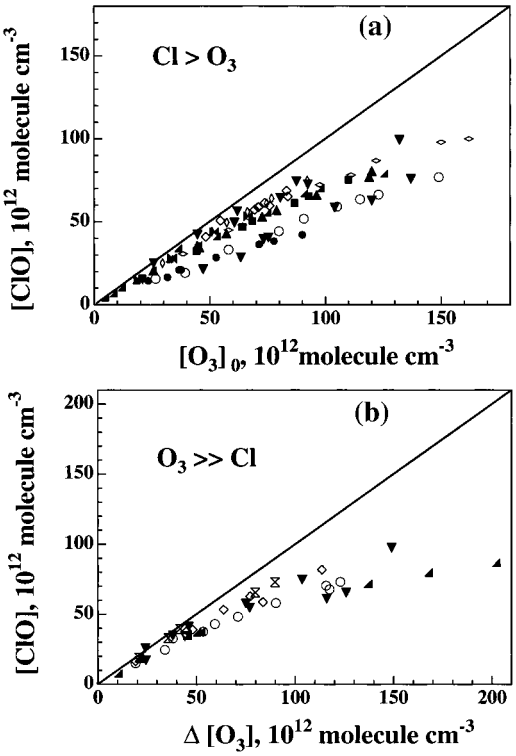

Figure 6. (a) Plot of the measure [ClO] vs $[O_3]_0$ obtained under conditions where O_3 was depleted during ClO production. (b) Plot of [ClO] vs $\Delta[O_3]$ for a few experiments done with O_3 in excess. Each of the symbols represents data taken during different days or under varying experimental conditions. If the production of ClO from O_3 were stoichiometric, the data points would fall on the 1-to-1 lines shown.

dependence.[3,8] In all of our experiments, the source region for ClO production was held at 298 K. Our experiments, along with those of Burkholder et al.[22] and Poulet et al.,[5] show that one cannot assume unit conversion of ozone to ClO, and those of Poulet et al.[5] showed that this was also true when reaction 19 was used to produce ClO.

Hills and Howard[3] were the first to report a negative temperature dependence ($k_1(T) = (8.0 \pm 1.4) \times 10^{-12}$ exp[(235 ± 46)] cm^3 molecule^{-1} s^{-1}) for reaction 1. They used a discharge−flow system with laser magnetic resonance capable of detecting OH, ClO, and HO_2, although not simultaneously. The rate coefficient was determined by measuring OH decays in an excess of ClO. The experiments were performed in a slight excess of O_3 to prevent the regeneration of OH from reaction of HO_2 with Cl. In general, the ClO concentration was calibrated from a plot of ClO signal vs $[O_3]_0$ obtained under conditions of excess Cl atoms and assuming $[ClO] = [O_3]_0$. As a test, Hills and Howard[3] verified the $[O_3]_0$ by converting it to NO_2 via reaction with NO,

$$O_3 + NO \rightarrow NO_2 + O_2 \qquad (21)$$

and compared the NO_2 signal to an absolute calibration for NO_2. Similarly, to test the accuracy of the ClO concentration obtained from the calibration plot, they converted ClO to NO_2 via reaction with NO,

$$ClO + NO \rightarrow NO_2 + Cl \qquad (22)$$

and compared the NO_2 signal to an absolute calibration for NO_2. Finally, they titrated ClO with small amounts of NO and observed the falloff in ClO signal as ClO was consumed. These tests showed that their ClO calibration should have been accurate within a few percent. As discussed earlier, we observed a wide range of conversion efficiencies for the production of ClO from O_3. Hills and Howard[3] did not observe this affect with ClO concentrations of $(0.14-1.25) \times 10^{13}$ molecule cm^{-3}.

Poulet et al.[5] measured k_1(298 K) using a discharge−flow system and laser-induced fluorescence to detect OH and mass spectrometry to detect ClO and HCl. They measured k_1 in three different ways. The first measurement was relative to the reaction

$$OH + OClO \rightarrow \text{products} \qquad (23)$$

where k_{23}(298 K) was first determined to be $(6.9 \pm 0.5) \times 10^{-12}$ cm^3 molecule^{-1} s^{-1}. Determination of k_1 required correction (∼28%) for the regeneration of OH via reaction 3a and yielded a value of $k_1 = (1.77 \pm 0.33) \times 10^{-11}$ cm^3 molecule^{-1} s^{-1}. In the second method, ClO was generated via reactions 2 or 9 in an excess of Cl atoms. ClO was titrated with NO and the resulting NO_2 signal compared to a calibrated NO_2 signal to determine [ClO], as in the experiment by Hills and Howard.[3] Again, this required correction (∼28%) for the regeneration of OH and yielded a value of $(1.99 \pm 0.25) \times 10^{-11}$ cm^3 molecule^{-1} s^{-1}. In the third method, ClO was made via reaction 2 with a slight excess of O_3. In these experiments ClO was not titrated with NO because the Cl atoms produced (reaction 22) can react to regenerate ClO (reaction 2) and because NO reacts with O_3 to produce NO_2. Instead, a mass spectrometric calibration of ClO was used to determine [ClO]. However, for this calibration, Cl atoms were added until the O_3 signal disappeared, and then it was assumed that $[ClO] = [O_3]_0$. From this experiment they obtained k_1(298 K) $= (1.89 \pm 0.21) \times 10^{-11}$ cm^3 molecule^{-1} s^{-1}.

Both Poulet et al.[5] and Hills and Howard[3] report values for k_1 larger than those from any previous experiments. Each of these groups carefully chose their experimental conditions to avoid complications from secondary chemistry and tested for the accuracy of their ClO concentration. Although these measurements do overlap within the 2σ uncertainties of one another, our measured k_1(298 K) in excess O_3 is larger than their reported values by ∼20% and ∼30%, respectively. A possible source for a systematic discrepancy could be the necessity of both groups to calibrate [ClO] under conditions of a slight excess of Cl atoms while measurements of k_1 were performed under conditions of excess O_3. If there were a systematic error in the ClO calibration, this could also affect other rate coefficients that relied on a similar calibration.[23]

More recently, Lipson et al.[8] used the turbulent flow technique with chemical ionization mass spectrometry to measure k_1 and report a value $k_1(T) = (5.5 \pm 1.6) \times 10^{-12}$ exp[(292 ± 72)] cm^3 molecule^{-1} s^{-1}. In their experiments, ClO was generated from reaction 2. The ClO signal was calibrated with NO via reaction 22, and ethane was added to the scavenge Cl atoms,

$$Cl + C_2H_6 \rightarrow HCl + C_2H_5 \qquad (24)$$

preventing regeneration of ClO from reaction 2. As they noted, one complication with this titration is that NO_2 can react with C_2H_5 formed in reaction 24:

$$NO_2 + C_2H_5 \rightarrow \text{products} \qquad (25)$$

They modeled this titration system to correct for the underestimation of the ClO concentration and report that the correction factor was almost always <15%. Simulation of this titration scheme requires accurate knowledge of the concentrations of

NO, ClO, OH, O_3, Cl_2, Cl, and C_2H_6 for each temporal profile. Therefore, we were unable to evaluate the model used in their titration scheme.

From the enthalpies of formation,[2] $\Delta_f H°_{298}$, and k_{3a} of $(9.1 \pm 1.3) \times 10^{-12}$ cm^3 molecule^{-1} s^{-1}, we calculated $\Delta_f H°_{298}$(HO$_2$) to be 3.0, 3.2, 3.1, and 3.3 kcal mol^{-1}, respectively, using k_1 measured by us, Hills and Howard,[3] Poulet et al.,[5] and Lipson et al.,[8] respectively. For this calculation the channel producing HCl was neglected, since it is, at most, a minor channel. These values all lie within the currently accepted value of (2.8 ± 0.5) kcal mol^{-1}, although the value of Lipson et al.[8] is at the limit of the uncertainty. Although our value of k_1 is higher than previously reported values, it is consistent with the enthalpy of formation for HO$_2$.

This is the first measurement of k_1 where [ClO] was determined by its absorption spectrum. The value determined here is larger than those reported previously. Our in situ measurement of [ClO] by UV/visible absorption eliminated the need to titrate ClO to determine its concentration. Therefore, it appears that our value of k_1 is accurate. Dubey et al.[1] recently showed (using a smaller rate coefficient than was measured in this work) that a branching ratio for channel 1b as small as 7% could be significant in the chlorine partitioning in the middle and upper stratosphere. By use of our rate coefficient, a similar influence could be achieved with a much smaller branching ratio for channel 1b. Other implications of the larger value of k_1 await analysis by modeling studies.

Acknowledgment. This work was funded in part by NASA Upper Atmospheric Research Program. This work constituted part of the Ph.D. thesis submitted by C. S. K.-O. to the University of Colorado, Boulder.

References and Notes

(1) Dubey, M. K.; McGrath, M. P.; Smith, G. P.; Rowland, R. S. *J. Phys. Chem. A* **1998**, *102* 3127.

(2) DeMore, W. B.; Sander, S. P.; Golden, D. M.; Hampson, R. F.; Kurylo, M. J.; Howard, C. J.; Ravishankara, A. R.; Kolb, C. E.; Molina, M. J. *Chemical Kinetics and Photochemical Data for Use in Stratospheric Modeling*; Jet Propulsion Laboratory: Pasadena, CA, 1997.

(3) Hills, A. J.; Howard, C. J. *J. Chem. Phys.* **1984**, *81*, 4458.

(4) Burrows, J. H.; Wallington, T. J.; Wayne, R. P. *J. Chem. Soc., Faraday Trans. 2* **1984**, *80*, 957.

(5) Poulet, G.; Laverdet, G.; LeBras, B. *J. Phys. Chem.* **1986**, *90*, 159.

(6) Leu, M. T.; Lin, C. L. *Geophys. Res. Lett.* **1979**, *6*, 425.

(7) Ravishankara, A. R.; Eisele, F. L.; Wine, P. H. *J. Chem. Phys.* **1983**, *78*, 1140.

(8) Lipson, J. B.; Elrod, M. J.; Beiderhase, T. W.; Molina, L. T.; Molina, M. J. *J. Chem. Soc., Faraday Trans.* **1997**, *93*, 2665.

(9) Turnipseed, A. A.; Gilles, M. K.; Burkholder, J. B.; Ravishankara, A. R. *J. Phys. Chem. A* **1997**, *101*, 5517.

(10) Baulch, D. L.; Cox, R. A.; Crutzen, P. J.; Hampson, R. F., Jr.; Kerr, J. A.; Troe, J.; Watson, R. T. *J. Phys. Chem. Ref. Data* **1982**, *11*, 373.

(11) Turnipseed, A. A.; Vaghjiani, G. L.; Thompson, J. E.; Ravishankara, A. R. *J. Chem. Phys.* **1992**, *96*, 5887.

(12) Davis, H. F.; Lee, Y. T. *J. Phys. Chem.* **1996**, *100*, 30.

(13) Vaghjiani, G. L.; Ravishankara, A. R. *J. Phys. Chem.* **1989**, *93*, 1948.

(14) Cady, G. H. *Inorg. Synth* **1957**, *5*, 156.

(15) Gilles, M. K.; Burkholder, J. B.; Ravishankara, A. R. *Int. J. Chem. Kinet.*, in press.

(16) Gilles, M. K.; Turnipseed, A. A.; Burkholder, J. B.; Ravishankara, A. R.; Solomon, S. *J. Phys. Chem. A* **1997**, *101* 5526.

(17) Lee, Y. P.; Howard, C. J. *J. Chem. Phys.* **1982**, *77*, 746.

(18) Burrows, J. P.; Cliff, D. I.; Harris, G. W.; Thrush, B. A.; Wilkinson, J. P. T. *Proc. R. Soc. London* **1979**, *A368*, 463.

(19) Cattell, F. C.; Cox, R. A. *J. Chem. Soc., Faraday Trans. 2* **1986**, *82* 1413.

(20) Dobis, O.; Benson, S. W. *J. Am. Chem. Soc.* **1993**, *115*, 8798.

(21) Malleson, A. M.; Kellett, H. M.; Myhill, R. G.; Sweetenham, W. P. *FACSIMILE*.; A. E. R. E. Harwell Publications Office: Oxfordshire, 1990.

(22) Burkholder, J. B.; Hammer, P. D.; Howard, C. J.; Goldman, A. *J. Geophys. Res.* **1989**, *94*, 2225.

(23) Stimpfle, R. M.; Perry, R. A.; Howard, C. J. *J. Chem. Phys.* **1979**, *71*, 5183.